Lesion Detection in Dermatoscopic Images Using Anisotropic Diffusion and Morphological Flooding

Philippe Schmid
Signal Processing Laboratory
Swiss Federal Institute of Technology
1015 Lausanne, Switzerland

Abstract

A new technique for the unsupervised detection of multiple objects in noisy background is presented in this paper, with application to digitized dermatoscopic images. The proposed method uses anisotropic diffusion in the $L^*u^*v^*$ uniform color space to suppress background noise and spurious structures while preserving the object boundaries. A simple and fast hair removal scheme based on morphological operators and luminance thresholding is also introduced for the application to pigmented skin lesions. The luminance component is then used to extract iso-level closed contours by morphological flooding. These curves are considered as contour candidates and the selection is based on the minimization of a gradient based energy functional. The main advantages of this technique is the low processing time and the possibility, if necessary, to scroll through the different level curves without additional processing.

1 Introduction

The research project we are working on must solve typical image analysis problems. Features must be extracted from medical images for diagnosis purpose, which implies the following three processing steps:

- filtering to remove artifacts and spurious components that may corrupt the following processing,
- the detection of the objects of interest through image segmentation or contour detection,
- the quantification of one or more features for the classification into different diagnostic classes.

The filtering step is essential to facilitate the following processing. It should prepare the image so that only the relevant (needed) information is preserved. If segmentation comes next, then ideally the filtering should smooth out regions and keep the boundaries intact. These two components are part of the contour detection scheme introduced in this paper.

The image processing techniques we develop are used for the diagnosis of malignant melanoma from dermatoscopic images. The slides are obtained by epiluminescence microscopy, a technique that uses an oil immersion to render the skin translucent, and then digitized for the computerized analysis.

In the following section I will briefly go through two pre-processing steps, namely the color space change and a simple scheme to remove hair from images. Anisotropic diffusion is presented in § 3.1 and extended to color images in § 3.2, morphological flooding is introduced in § 3.3, and an energy functional is defined in § 3.4. Finally examples are given in Section 4 and some conclusions are drawn in Section 5.

2 Pre-processing

2.1 Color space

The color space used for the processing of color images is a crucial choice. I generally suggest to use uniform color spaces, such as $L^*u^*v^*$ [1]. The main advantage is that color difference can be measured and used for comparisons between pixels or distance measures in the spectral domain. In our case this characteristic is very important for the diffusion part where the image gradient norm can be efficiently replaced by a color distance. This technique is introduced later.

Another advantage is the separation between the luminance and chrominance components. Luminance is very important in dermatoscopic images since it reflects every pigmented structure present in the lesion. In fact the coloring matter is the *melanin*, whose concentration and depth gives the impression of color. These two parameters define also how light is reflected and therefore reveal all the pigmented structures. This component will be used in the last stage to extract the iso-level contour lines.

2.2 Hair removal

The goal in this section is not to propose a way to restore hidden information due to the presence of hair but to replace the concerned image pixels in such a

0-7803-5467-2/99/ $ 10.00

way that later processing is not influenced. It must be clearly underlined here that any spurious detail introduced at the acquisition level is definitely present and that there is no way to "repair" the image. It is however possible to detect these components and to reduce the (negative) visual effect they cause, which in turn deteriorates the medical diagnosis.

The approach I suggest is to apply the morphological closing operator [2] with a spherical structuring element to the luminance component L^* and to threshold the difference with the original image. Hair is indeed very light absorbent and we could experience that a constant threshold can be set up quickly, even when the image "quality" is variable. The selected pixels are replaced with their value after the closing operation, while other pixels are left unchanged. It may happen that part of pigmented structures show to have a similar morphology and a high contrast, but even if part of them are selected as hair, the introduced modification is usually imperceptible and without effect on the following filtering.

3 Contour detection

3.1 Anisotropic diffusion

The filtering technique used in this study is anisotropic diffusion, also called nonlinear isotropic diffusion. The goal is to make pixel values diffuse in the image as heat does in matter. The great idea introduced by Perona and Malik [3] is to control the diffusion with a nonlinear *conductivity function* which is a monotically decreasing function of the gradient. The diffusion being still isotropic, this process is in fact a *nonlinear isotropic diffusion* even if in most of the related literature it is called *anisotropic diffusion.*

The basic diffusion equation is a *time-varying partial differential equation* (PDE):

$$\frac{\partial v}{\partial t} = \nabla \cdot (g(|\nabla v|)\nabla v) \ ,$$

where $v(\boldsymbol{x}, t) : \mathbb{Z}^2 \times \mathbb{R} \mapsto \mathbb{R}^n$ is the image value at position $\boldsymbol{x}$ and time t, and n is the data dimension. We suppose that the image is vector-valued and that a pixel value is a vector which may reduce to a scalar when the image is a gray level image, but which may also describe color or texture information. The conductivity function $g(|\nabla v|)$ which controls the diffusion must obey a number of conditions [4] in order to have a well-posed system and to avoid the convergence towards local steady-states. An equation that fulfills these conditions and that we will use in our scheme is given by:

$$g(|\nabla v|) = \begin{cases} 1 & \text{if } |\nabla v| \leq k_0, \\ k_0/|\nabla v| & \text{if } |\nabla v| > k_0. \end{cases} , \qquad (1)$$

where k_0 is a threshold value. This function is very simple to implement and has the advantage to never stop completely the diffusion. The consequence is that small impulse noise is smoothed out quickly because of the small surface it covers, despite the large gradient values it introduces. Equation (1) has a constant part for small gradient values in order to avoid infinite conductivities for null gradient.

More complex functions did not improve much the results, while requiring much more computation time. Tensor-driven diffusion [5], where the conductivity function is replaced by a *conductivity tensor*, has also been evaluated. The direction of diffusion can be controlled very precisely, which may be very interesting for some applications, but the computation time becomes very important and the results did not outperform what could be obtained with the scalar approach.

To illustrate the robustness of the conductivity function given by Eq. (1) we have computed the evolution of the *peak signal-to-noise ratio* (PSNR) for a dermatoscopic image corrupted with Gaussian noise and for increasing variance values. The original image diffuses in parallel and is used for the PSNR computation. The same procedure has been repeated with the following Perona-Malik function:

$$g(|\nabla \nu|) = \exp\left[-\left(\frac{|\nabla v|}{k_0}\right)^2\right] .$$

The results are shown in Fig. 1 for the Perona-Malik function and Fig. 2 for Eq. (1). They clearly show that the diffusion process using the proposed diffusion function has a strong noise removal effect.

3.2 Color diffusion

The mathematical formulation of anisotropic diffusion presented in the previous paragraph is for application to scalar images. The logical following step is the application to vector-valued images. A typical example of vector-value is color. The different components are linked by the conductivity function that becomes a function of the different gradients:

$$\frac{\partial v_i}{\partial t} = \nabla \cdot (g(|\nabla v_1|, \ldots, |\nabla v_d|)\nabla v_i) \ , \ i = 1, \ldots, n \ ,$$

while the diffusion itself is done separately for every component. It seems reasonable to control the diffusion according to the different gradients obtained from every image component. For color images for example, the blue component may have no large gradient at a specific location, while the color image shows clearly a transition. To make this edge visible, all three components must be taken into account in order to decide if the local structure is flat or not.

In [6] the complete paper deals with this problem. The proposed approach is based on the minimization of the *first fundamental form* through eigenvalue/eigenvector analysis in order to detect the direction of maximal variation. This technique however do not take into account the "weight" of the different components.

One can argue that the visual contribution of the different components is not always clear, especially for texture descriptors. In the case of color images, the use of uniform color spaces can provide a multi-dimensional gradient that fits the perceived color changes. Finally the diffusion of color images is done in the $L^*u^*v^*$ color space with $g(\sqrt{\sum_i |\nabla v_i|^2})$.

The combined color frame diffusion has the advantage, compared to the separate diffusion, to "mark" every component with the edge information contained in the two others. This morphological effect is very important for the next step, where one component must be kept to extract iso-level contours.

3.3 Morphological flooding

After the diffusion process only the luminance component is kept. It is considered in the following as a 3-D surface representation of the lesion. From this image all the iso-level contours are extracted by progressively flooding the image from the image frame pixels.

This process can be formulated as an iterative morphological operator using set theory. It is a particular operator, since the input image is a gray-scale image and the output at a given level is a binary image. It is therefore necessary to introduce some morphological operators for binary images. Let $\mathbb{A}$ and $\mathbb{B}$ be sets in $\mathbb{Z}^2$, with components $\boldsymbol{a}$ and $\boldsymbol{b}$ respectively. The *translation* of $\mathbb{A}$ by $\boldsymbol{x}$ is defined as:

$$(\mathbb{A})_{\boldsymbol{x}} = \{\boldsymbol{c} \in \mathbb{Z}^2 \mid \boldsymbol{c} = \boldsymbol{a} + \boldsymbol{x}, \quad \boldsymbol{a} \in \mathbb{A}\},$$

and the *reflection* of $\mathbb{B}$ is defined as:

$$\hat{\mathbb{B}} = \{\boldsymbol{x} \in \mathbb{Z}^2 \mid \boldsymbol{x} = -\boldsymbol{b}, \quad \boldsymbol{b} \in \mathbb{B}\}.$$

The *dilation* of $\mathbb{A}$ by $\mathbb{B}$ is defined as:

$$\mathbb{A} \oplus \mathbb{B} = \{\boldsymbol{x} \in \mathbb{Z}^2 \mid (\hat{\mathbb{B}})_{\boldsymbol{x}} \cap \mathbb{A} \neq \emptyset\} .$$

With these three definitions we can now give a set formulation to the morphological flooding. Let the input image be described by a function $v(\boldsymbol{x}) : \mathbb{Z}^2 \mapsto \mathbb{R}$, with $\mathbb{D}_v$ the image domain and $\partial\mathbb{D}_v$ the image border domain. The following operator is used to build the subset of flooded pixels at level $l \in \mathbb{R}$:

$$\mathbb{F}_k^{(l)} = (\mathbb{F}_{k-1}^{(l)} \oplus \mathbb{B}) \cap \{\boldsymbol{x} \in \mathbb{D}_v \mid v(\boldsymbol{x}) \leq l\} \ , \ k \in \mathbb{N}^* \ ,$$

where $\mathbb{B}$ is a structuring element, usually a cross (4-connected) or a 3×3 square (8-connected). The operator is initialized for $k = 0$ as follows:

$$\mathbb{F}_0^{(l)} = \{\boldsymbol{x} \in \partial\mathbb{D}_v \mid v(\boldsymbol{x}) \leq l\} \ ,$$

and it has converged when $\mathbb{F}_k^{(l)} = \mathbb{F}_{k-1}^{(l)}$ and we let then $\mathbb{F}^{(l)} = \mathbb{F}_k^{(l)}$ be the set of pixels flooded at level l.

It is straightforward that the complete procedure is not repeated for every level and that for $l_2 > l_1$ the flooded subset for level l_2 is obtained by starting the flooding with the result obtained at level l_1. The only condition is that:

$$\mathbb{F}_0^{(l_2)} = \mathbb{F}^{(l_1)} \cup \{\boldsymbol{x} \in \partial\mathbb{D}_v \mid v(\boldsymbol{x}) \leq l_2\} \ .$$

The above equation ensures that flooding can start at local border minima. The flooding process provides a kind of 2-D *convex hull* of the gray level image, which has the following feature: *there always exist a convex path between the image border and any point in the image.* This hull is obtained with the different subsets $\mathbb{F}^{(l_i)}$, $i \in \mathbb{N}^*$ and $\cup_i \mathbb{F}^{(l_i)} \equiv \mathbb{D}_v$, by labeling every image pixel in $\mathbb{D}_v$ according to the following rule:

$$h(\boldsymbol{x}) = l_0 \ , \quad \forall \boldsymbol{x} \in \mathbb{F}^{(l_0)} \ ,$$

and

$$h(\boldsymbol{x}) = l_i \ , \forall \boldsymbol{x} \in \{\boldsymbol{x} \in \mathbb{F}^{(l_i)} \mid \boldsymbol{x} \ni \mathbb{F}^{(l_{i-1})}\} \ , i \in \mathbb{N}^* \ .$$

From this representation the different iso-level curves are extracted by simple image slicing. For every level an energy functional is evaluated on the contour pixels.

3.4 Energy functional

The iso-level curve energy is computed as follows:

$$\mathcal{E}_l = (1 + E[e(\mathcal{C}_l)]) \cdot (1 + Var[e(\mathcal{C}_l)]) \ ,$$

where $e(\mathcal{C}_l)$ is actually the energy measure, $E[e(\mathcal{C}_l)]$ is the expected or mean value along the curve at level l and $Var[e(\mathcal{C}_l)]$ is the corresponding variance. In order to select the curve with lowest energy and lowest energy variance the above equation is used. The unit offset in both parentheses ensure that if only one of the two measures is zero the resulting energy is non-zero.

The energy term $e(C_l)$ is taken equal to the conductivity function given be Eq. (1), with a squared gradient equal to the sum of the squared gradients of the different components L^*, u^*, and v^*, taking like that into account the color difference formula to measure color derivatives as color distances.

4 Results

An example of lesion after diffusion is given in Fig. 3 with some of the iso-level curves. The corresponding energy functional is plotted in Fig. 4, and the contour corresponding to the minimum energy is superimposed to the original lesion in Fig. 5.

In practice not only the lesion boundary can be extracted following this technique but also other regions that might correspond to relevant structures within the lesion, like globules for example. In that case not only the energy minimum is selected but also local minima, which requires that the energy functional has been smoothed out after its computation.

5 Summary and Conclusions

The contour detection scheme can be summarized as follows:

- change from *RGB* to $L^*u^*v^*$ color space,
- remove hair using the scheme introduced in § 2.2,
- use color anisotropic diffusion to smooth out small components and spurious details,
- use morphological flooding to extract iso-level contours from the luminance component,
- compute a gradient based energy functional to select the best fitting curve.

We could visually assess the results for more than 300 mixed lesions of variable "quality". The results are very promising, even when the image is corrupted by hair. This method has the advantage of being very fast compared to other methods which use diffusion for segmentation or contour detection purpose (geodesic snakes for example). The number of iterations in the diffusion process is much smaller and the flooding allows for the detection of closed contours. Even in the presence of multiple lesions this method succeeds. Finally, a friendly graphical user interface will allow the physician, if necessary, to fine tune the contour selection using a scroll bar.

Acknowledgments

The author would like to thank Dr. J. Guillod from the Centre Hospitalier Universitaire Vaudois (CHUV) for his help and for providing the test images, and Prof. M. Kunt for supporting this project.

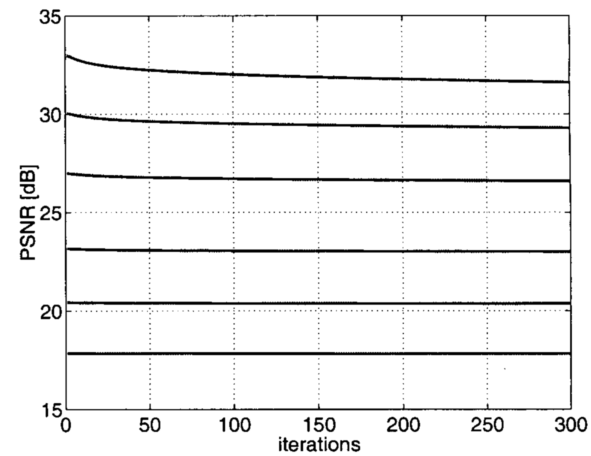

Figure 1: Variation in time (iterations) of the PSNR in noisy environment. The different curves, from bottom to top, correspond to additional Gaussian noise with zero mean and decreasing variance. The conductivity function is the decreasing exponential proposed by Perona and Malik [3].

References

[1] G. Wyszecki and W. S. Stiles, *Color science: concepts and methods, quantitative data and formulae*, Wiley, 1982.

[2] R. C. Gonzalez and R. E. Woods, *Digital Image Processing*, Addison-Wesley, 1993.

[3] P. Perona and J. Malik, "Scale-space and edge detection using anisotropic diffusion", *IEEE Transactions on Pattern Analysis and Machine Intelligence*, vol. 12, no. 7, pp. 629-639, 1990.

[4] Y.-L. You, W. Xu, A. Tannenbaum and M. Kaveh, "Behavioral analysis of anisotropic diffusion in image processing", *IEEE Transactions on Image Processing*, vol. 5, no. 11, pp. 1539-1553, 1996.

[5] J. Weickert, "Anisotropic diffusion in image processing", *Ph.D. thesis*, Universität Kaiserslautern, 1996.

[6] G. Sapiro and D. L. Ringach, "Anisotropic diffusion of multivalued images with applications to color filtering", *IEEE Transactions on Image Processing*, vol. 5, no. 11, pp. 1582-1586, 1996.

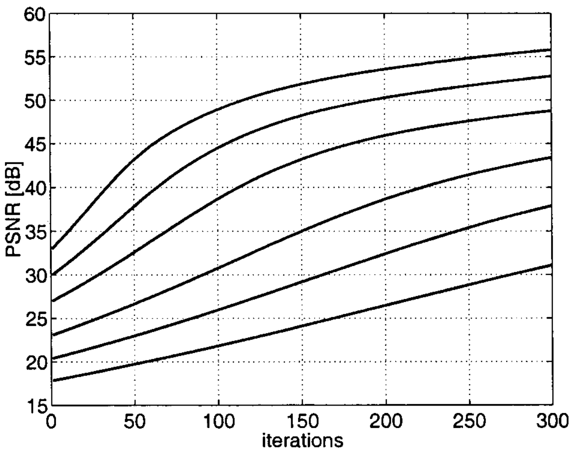

Figure 2: In this example the (well-posed) proposed conductivity function is used, rendering the system very noise resistant.

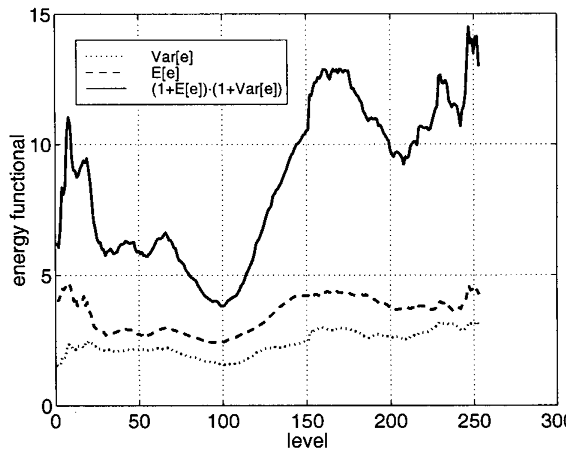

Figure 4: Energy curve obtained from the morphological flooding. The minimum correspond to the lesion boundary.

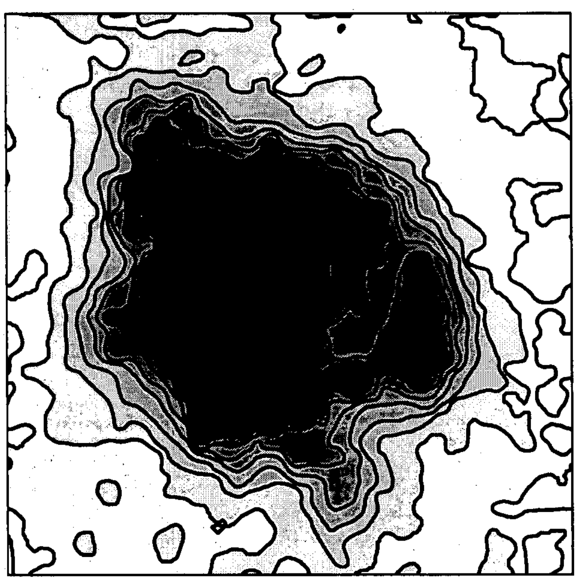

Figure 3: This image shows a pigmented lesion after color diffusion and morphological flooding. Some of the obtained contour lines are shown as black lines.

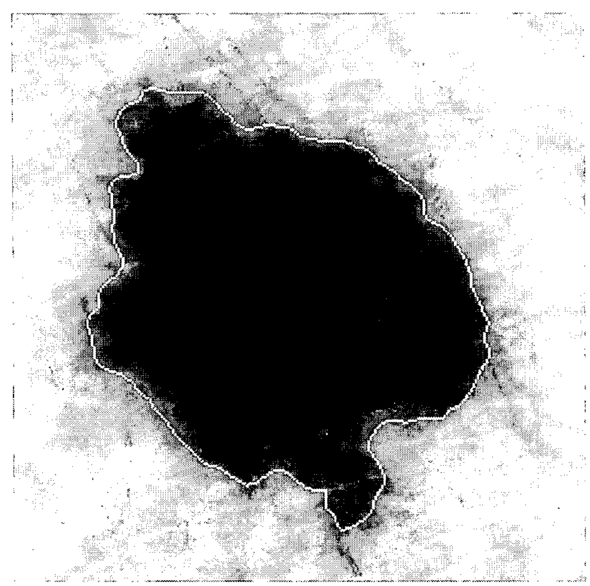

Figure 5: Pigmented skin lesion with the superimposed contour obtained through the detection scheme introduced in this paper.